THE EXPERIMENT
INTERNATIONAL JOURNAL OF SCIENCE AND TECHNOLOGY

ISSN-2319-2119

RESEARCH ARTICLE

R.J Waltman , *TheExperiment,2017,Vol42(2),2428-2440*

Boundary Lubricant Film Properties of Z-Tetraol Modified by Benzene Rings

Abstract:
The adsorbed film structures of perfluoropolyethers (PFPEs) modified with benzene functional group(s) either on the chain ends or in the middle of the main chain are investigated. Surface energy as a function of PFPE film thickness and of time shows the benzene functional group orients towards the carbon surface (CNx). The re-orientation is kinetically much slower than for hydroxyl end groups for PFPEs having similar main chain compositions. The bonding of the benzene functional group to the underlying CNx surface is significantly weaker than OH functional groups and/or more readily removed by the solvent used to originally deposit the PFPE film onto the carbon surface. Model dimer interactions via ab initio computational chemistry calculations shows a significantly longer closest contact distance for the benzene/CNx dimer compared to OH/CNx dimer, indicative of the weaker intermolecular interaction.

Keywords: Boundary lubricant; Perfluoropolyether; Benzene functional groups; Lubricant bonding; surface energy; Dimer interactions.

Introduction:
In the computer disk industry, hydroxyl-terminated perfluoropolyethers (PFPEs) have served as the ultra-thin boundary lubricant film of choice for over 20 years. During this time considerable evolution of the PFPE chemical structures has occurred to meet the tribological challenges of the reduced mechanical spacing between the read/write pole tip of the low-flying slider and the disk surface. Central to the advancement of these newer PFPEs was the recognition that the main chain itself was the significant determinant [1, 2]. Thus optimization of dynamic loop-to-train ratio, two-dimensional persistence length, packing density, and mobility has allowed PFPEs to keep pace with technological development. One significant evolution was the development of a multi-functional PFPE called “ZTMD” which contained four hydroxyl groups on the chain ends and four more in the middle of the main chain [3]. While this chemical structure significantly reduced lubricant transfer from disk to slider its more solid-like properties exacerbated slider wear rate.

It is desirable to reduce the severity of the contact wear problem associated with PFPEs like ZTMD by reducing its solid-like properties whilst retaining the tribological benefits of a PFPE design incorporating multi-functionality. One possibility is to replace some or all of the OH groups that bind to the underlying carbon surface with benzene rings. The first non-vanishing permanent electrical moment of benzene is a quadrupole. Consequently, dimer interactions between benzene and the underlying carbon surface will be weaker than for end groups like hydroxyl which have a dipole or which have the ability to form hydrogen bonds. Benzene’s quadrupole, associated with a negative charge density of the π clouds both above and below the plane of the molecule, are capable of π/π, π/OH, π/NH and π/CH interactions having weaker intermolecular interaction energies of approximately 2 – 3 kcal/mol compared to OH/OH and OH/NH intermolecular interaction energies of approximately 5 – 6 kcal/mol [4]. Since the “bonding” of PFPE end groups to the underlying carbon surface is a required property of PFPEs in computer disk applications, it is of great interest to ascertain how well benzene functional groups can fulfill this requirement.

Materials and Methods:
Z-Tetraol (Mn 2200) and Zdol (Mn 2500) were obtained from Solvay-Solexis and used directly. A sample of “ZTB” having a central benzene ring between two tetraol-terminated perfluoropolyether chains was kindly provided by Moresco (Japan).The benzene-terminated analog of Z-Tetraol, hereafter referred to as

THE EXPERIMENT
INTERNATIONAL JOURNAL OF SCIENCE AND TECHNOLOGY

ISSN-2319-2119

RESEARCH ARTICLE

R.J Waltman , *TheExperiment,2017,Vol42(2),2428-2440*

"ZB2", was synthesized directly from Zdol 2500 [5]. The chemical structures are shown in Fig. 1. NMR data for the three PFPE lubricants are summarized in Table 1.

The substrates used in these studies were 65 mm diameter glass disks of nominally 2 Å RMS roughness as measured by a Dimension 5000 AFM using a standard AFM tip in the tapping mode. The typical scan size for these measurements was 1 μm x 1 μm with a scan rate of 0.5 Hz and 256 lines of resolution. Atop the substrates a cobalt-based magnetic recording layer (CoPtCr) was sputter-deposited, followed by CVD deposition of 30 Å of an amorphous nitrogenated carbon film (called "CNx") comprised nominally of 15 to 20 atomic percent (at%) N.

The perfluoropolyether (PFPE) lubricant films were applied to the carbon surfaces from solvent using a standard dip-coating methodology, using a typical concentration of 0.05 g/liter and a typical disk withdrawal rate of several mm/sec. The thicknesses of the topically applied PFPE lubricant films were quantified by specular reflection FTIR (Nicolet Magna Model 560). The FTIR absorption band maximum for each PFPE was in turn correlated to film thickness by XPS (Phi Quantum 2000 ESCA System) using a takeoff angle of 45^o and an electron mean free path of 25 Å [6]. The FTIR-ESCA thickness correlation is shown in Fig. 2. The PFPE bonded fraction was quantified by rinsing the disks in Vertrel-XF solvent for 1 min then normalizing the measured remaining film thickness to the initial film thickness. Surface energy measurements were accomplished by contact angle goniometry using hexadecane (γ_l^d = 27.5 mJ/m^2) and water (γ_l^d = 21.8 mJ/m^2, and γ_l^p = 51.0 mJ/m^2) as the reference liquids. Information on the monolayer and dewetting film thicknesses of the PFPE films were obtained by directly imaging the disk surface ellipsometrically for lubricant droplets and by identifying the surface energy minimum by contact angle goniometry. An optical surface analyzer (OSA) using both s- and p-polarized light was employed to directly image the disk surface for evidence of lubricant dewetting.

Computational Methods:

Ab initio calculations were performed using either MP2 or density functional theory (DFT) at the 6-311++G(d,p) basis set using the Gaussian 98 computer code [7]. The DFT calculations employed Becke's 3-parameter functional together with Perdew and Wang's gradient-corrected correlation functional [8, 9]. The 6-311++G(d,p) basis set includes *d* functions for oxygen atoms and *p* functions for hydrogen atoms, both of which allow a more quantitative description of hydrogen bonding. All model structures were fully optimized. The requested convergence on the density matrices was 10^{-8}. Residual forces were $\leq 1 \times 10^{-4}$ hartree bohr^{-1} on the cartesian components. Harmonic vibrational frequencies were calculated by differentiation of the energy gradient at the optimized geometry. No imaginary frequencies were computed for all structures. The figures reproducing the computational results were made using the Gauss View graphical user interface [10] and the Cambridge Soft graphical software [11].

The strength of the bonding interaction between the polar OH group of the PFPE and either the carbon surface, the Vertrel-XF solvent, or another PFPE molecule was quantified by dimer calculations on representative model structures. In order to keep the computations tractable, the PFPE OH was represented by HCF_2CH_2OH (Zdol end group) whilst the CNx carbon surface was represented by the imine $CH_3N{=}CH_2$. The Vertrel-XF structure was represented by the authentic $CF_3CHFCHFCF_2CF_3$ formula. The computed binding energy is obtained as the difference in total energies between the dimer and the isolated reactants, i.e., $\Delta E = E_{AB} - (E_A + E_B)$, corrected for zero-point energy contributions.

The strength of the bonding interaction between ZB2 and the carbon surface or the Vertrel-XF solvent was also quantified by dimer calculations. Here only MP2 calculations are reported. In order to keep the computations tractable, the ZB2 end group was represented by benzene whilst the CNx carbon surface was represented by the amine $(CH_3)_3N$. The Vertrel-XF structure was represented by CH_3F. The computed

THE EXPERIMENT
INTERNATIONAL JOURNAL OF SCIENCE AND TECHNOLOGY

ISSN-2319-2119

RESEARCH ARTICLE

R.J Waltman , *TheExperiment,2017,Vol42(2),2428-2440*

binding energy was obtained as the difference in total energies between the dimer and the isolated reactants corrected for zero-point energy contributions. No corrections for basis set superposition error (BSSE) were made here [12]. According to the literature the main consequence is an overestimation of the interaction energy. Since MP2 itself may also overestimate the interaction energy, the computed interaction energy reported here at the MP2 level of theory is expected to be significantly larger than what is considered to be accurate in the literature [4]. Therefore we focus on the optimized dimer geometries and compare the intermolecular distances for the computed polar dimers.

Results and Discussion:

The adhesion of the PFPE boundary lubricant films to the underlying carbon surface is quantified by the bonding kinetics. Fig. 3a shows the bonding kinetics for 10 Å Z-Tetraol, ZTB and ZB2 on CNx at 20 ºC and 50 % RH. Upon application of the lubricant films to the carbon surface, a fraction of the lubricant bonds at room temperature within the time required to allow for solvent evaporation and to conduct the initial thickness measurements. The initial bonded fraction is significantly larger for Z-Tetraol and ZTB than ZB2. All of the PFPEs exhibit increasing bonding to the CNx surface with increasing time. Z-Tetraol and ZTB reach an asymptotic bonded fraction of approximately 0.6 – 0.7 whilst ZB2 reaches a significantly smaller bonded fraction of 0.2 after the same time. These data are indicative that the benzene functional moiety does not provide as strong bonding as the OH groups to the underlying carbon film. Since the carbon films have surface functional groups such as OH and amines or imines, the Z-Tetraol and ZTB OH groups can hydrogen bond with the relatively stronger intermolecular interaction energies of approximately 5 – 7 kcal/mol [4]. ZB2, truncated by phenyl rings, is capable only of the weaker π/π, π/OH, π/NH and π/CH intermolecular interactions and are therefore not as strongly adhered. These weaker intermolecular interaction energies are typically 2 – 3 kcal/mol [4].

Conclusions on the relative adhesive strengths of the PFPEs to the underlying CNx surface based on the bonded fraction alone suffers from an additional complication. Since the bonded fraction is determined by a solvent rinse, we suspect that the strength of the solvent interaction with the PFPE lubricant relative to the PFPE/CNx interaction strength may also be a determinant. We discuss some of these aspects below utilizing ab initio dimer calculations on model PFPE/CNx and PFPE/solvent interactions. We consider first the polar interactions between PFPE end groups and the CNx and solvent surfaces. The relative strength of the intermolecular interaction between a PFPE OH end group and a model CNx carbon surface imine ($CH_3N{=}CH_2$), another PFPE OH end group, and the Vertrel-XF solvent. The goal of this theoretical study is to quantify the relative interaction strength between the PFPE OH end group and model surfaces and hence provide insight into the effect of solvent power on the bonding measurements. The optimized geometries for the interacting dimers are shown in Fig. 4. OH/imine and OH/OH interactions are consistent with hydrogen bonding characterized by the 1.8 Å closest contact distance. The OH/Vertrel-XF interaction is characterized by a significantly longer 2.2 Å closest contact distance. The computed binding energies and hydrogen bond distances are summarized in Table 2. As shown in Table 2, the PFPE OH dimer binding energy decreases in the order: imine > PFPE OH > Vertrel-XF. It is reasonable to conclude from the computational results that Vertrel-XF can more easily dissolve Tetraol molecules with “free” hydroxyls while the dissolution of a Tetraol hydroxyl bonded either to another Tetraol hydroxyl or to a polar group on the carbon surface becomes increasingly energetically prohibitive, respectively. This is consistent with the increasing bonded fraction of Z-Tetraol and ZTB as a function of time, Fig. 3a, and the more limited solubility of Z-Tetraol and ZTB in a solvent like Vertrel-XF compared to non-functionalized PFPEs.

Fig. 5 shows the model optimized geometries for ZB2/CNx (left) and ZB2/Vertrel-XF (right) using the benzene/$(CH_3)_3N$ and benzene/CH_3F dimers, respectively. For the benzene/ $(CH_3)_3N$ dimer, the amine nitrogen sits above the center of the benzene ring with a relatively large intermolecular close contact distance of 3.0 Å. The lone pair is pointed towards the benzene which creates a repulsive intermolecular

THE EXPERIMENT
INTERNATIONAL JOURNAL OF SCIENCE AND TECHNOLOGY

ISSN-2319-2119

RESEARCH ARTICLE

R.J Waltman , *TheExperiment,2017,Vol42(2),2428-2440*

interaction. For the benzene/CH_3F dimer, the CH_3F hydrogen sits above the center of the benzene ring with an intermolecular close contact of 2.5 Å. This is the typical dimer geometry when benzene acts as a proton acceptor [4].The computed binding energies and closest contact distances are summarized in Table 3. Unlike the polar interactions, the intermolecular closest contact distances are much larger than those computed for hydrogen bonding (Fig. 4). The ZB2/CNx and benzene/CH_3F binding energies, -5.2 and -4.4 kcal/mol, respectively, are likely to be substantially overestimated (no BSSE correction; no electron correlation beyond MP2; basis set effect) so no comparison to the polar interaction energies (Table 2) are made here [4]. Based on closest contact distances, the expectation is that the benzene functional moiety adheres less strongly than the polar OH, consistent with the observed bonding kinetics (Fig. 3). Finally, Fig .5 (middle) shows the model optimized geometry for the methoxybenzene/CNx dimer. As found for the benzene/$(CH_3)_3N$ dimer (Fig. 5 left), the amine nitrogen sits very close to the center of the benzene ring with a still relatively large intermolecular close contact distance of 3.0 Å. Consequently, the addition of an electron-donating methoxy substituent on benzene is not expected to improve binding to the underlying CNx surface.

According to the discussions above, it appears that the more polar PFPE molecules (Z-Tetraol; ZTB) could have more limited solubility in Vertrel-XF compared to ZB2. It is possible that the more polar PFPE lubricant components are more readily deposited from a "poorer" solvent and, once deposited on the disk, are not as easily re-dissolved in the solvent, thereby influencing the bonded fraction. Solubility originates from the interaction energy between the solute and the solvent. The solubility parameter is defined as the square root of the cohesive energy density [13]:

$$\delta_i = \sqrt{\frac{\Delta E_i^{\,v}}{V_i}} \qquad (\text{cal/cm}^3)^{1/2} \qquad (1)$$

ΔE_i^v is the energy of vaporization and V_i is the molar volume of component i.The solubility parameter, δ, therefore describes the attractive strength between molecules and can be used as a criterion for the solvent power. Eq. 1 is related to the heat of mixing per unit volume as [13]:

$\Delta H_m/V = (\delta_1 - \delta_2)^{1/2}\varphi_1\varphi_2$ (2)

φ_i is the volume fraction of component i. Since the free energy of mixing is related to the enthalpy of mixing by $\Delta G_m = \Delta H_m - T\Delta S_m$, the difference in the polymer-solvent solubility parameter $(\delta_1 - \delta_2)$ must be small for miscibility. The solubility parameter is conveniently calculated by expanding ΔE^v and V as [14]:

$\Delta E^v = \Sigma\, \Delta e_j$ (3)

and

$V = \Sigma\, \Delta v_j$ (4)

Δe_j and Δv_j are the additive atomic and group contribution for the energy of vaporization and molar volume, respectively. The computed solubility parameter for Z-Tetraol and ZB2 as a function of molecular weight is shown in Fig. 6. Table 4 compares the solubility parameters for Z-Tetraol, ZB2 and Vertrel-XF at the relevant molecular weights. Table 4 clearly shows that the enthalpy of mixing does not favor the solution of the more polar PFPEs as indicated by the solubility parameter $(\delta_1 - \delta_2)$. Thus ZB2 is expected to be considerably more soluble in Vertrel-XF than is Z-Tetraol. These data indicate that PFPEs with increasing polarity, i.e., more OH groups and/or lower molecular weight, are more likely to deposit onto the carbon surface. These polar adducts are also less likely to re-dissolve in the solvent upon hydrogen bonding to the underlying carbon surface, giving rise to an apparently larger initial bonded fraction. It is important to state that the lower bonded fraction for ZB2 (Fig. 3) does not necessarily exclude the benzene end groups from having oriented on the CNx surface for favorable physisorption (Fig. 5). It only means that the solvent interaction is capable of removing more of it from the surface. The concomitant changes in the polar

THE EXPERIMENT
INTERNATIONAL JOURNAL OF SCIENCE AND TECHNOLOGY

ISSN-2319-2119

RESEARCH ARTICLE

R.J Waltman , *TheExperiment,2017,Vol42(2),2428-2440*

surface energy as a function of time, Fig. 3b, measured simultaneously with the bonding kinetics (Fig. 3a), shows the surface reconstruction of the PFPE films on the CNx surface as evidenced by the decreasing γ_s^p with time. For Z-Tetraol and ZTB with the polar OH end groups, the polar surface energy decreases with time as observed previously [15]. This is attributed to the preferential interaction of the OH end groups to the polar functional groups of the underlying carbon surface, orienting the perfluoropolyether backbone to the air/PFPE interface. ZB2 also exhibits a similar surface reconstruction with the benzene end group only significantly smaller in magnitude and rate (Fig. 3b).

Additional information on the adsorbed PFPE film structures can be elucidated from their surface energy as a function of PFPE film thickness. The dispersive surface energy $\gamma_s^d(h)$ as a function of film thickness is compared for Z-Tetraol, ZTB and ZB2, Fig. 7a. For Z-Tetraol, $\gamma_s^d(h)$ is observed to decrease monotonically with increasing film thickness asymptotically approaching the bulk value of about 14 mJ/m^2. Conversely, $\gamma_s^d(h)$ for ZTB and ZB2 both exhibit a local minimum which is indicative that the benzene end groups preferentially locate at the carbon surface up to the monolayer film thickness. The ZTB and ZB2 film thickness at the γ_s^d minimum is approximately 17 to 18 Å. Once the monolayer film thickness is exceeded, the benzene rings preferentially orient towards the air interface causing $\gamma_s^d(h)$ to increase.

The corresponding polar surface energy, γ_s^p, as a function of film thickness is shown in Fig. 7b. Here significant differences are observed for Z-Tetraol and ZTB versus ZB2. First, a distinct oscillation in γ_s^p as a function of film thickness is observed only for Z-Tetraol and ZTB, both of which chemical structures are truncated by OH groups (Fig. 1). The oscillations are indicative of molecular layering in the PFPEs induced by the polar interactions of the PFPE OH end groups with the underlying carbon surface, much as observed previously [15]. The decrease in γ_s^p as a function of film thickness within the first PFPE monolayer is due to the PFPE backbone at the air/PFPE interface. In the next layer, γ_s^p increases because the PFPE OH end groups cannot access the underlying carbon surface and thus populates the air/PFPE interface. As shown in the figure, the structuring is propagated through several or more layers. The first minimum corresponds to the film thickness at which the surface becomes saturated with lubricant, i.e., the monolayer film thickness, which is approximately 20 Å for Z-Tetraol and 18 Å for ZTB. The magnitude of γ_s^p as a function of film thickness depends upon both the bonded fraction at the time of measurement and the atomic % N in the CNx film, both of which are not the focal point of these studies. Conversely, ZB2 shows no minimum in γ_s^p as a function of film thickness, indicative that strong adhesion between the benzene end group and the carbon surface has not taken place. Since the bare carbon film has a γ_s^p of approximately 40 mJ/m^2, it is reasonable to assume that the water droplets used to measure the contact angle displace the ZB2 film due to a lack of strong intermolecular adhesion (ZB2/CNx) and cohesion (ZB2/ZB2), Fig. 7b.

Ellipsometric imaging of the ZTB and ZB2 films as a function of film thickness was used to corroborate the monolayer film thicknesses identified by the surface energy data. Z-Tetraol has been discussed previously [15]. As shown in Fig. 8, ZTB and ZB2 films having thicknesses $\leq$ ~ 18Å are contiguous and display no signs of dewetting. However, when the ZTB and ZB2 film thicknesses are increased above their monolayer thickness, the thermodynamic instability causes the formation of lubricant “droplets” which are readily observed as the darker spots on the imaged surfaces. The monolayer film thicknesses from the surface energy and ellipsometric imaging are summarized in Table 5.

PFPE structures based on ZB2 with phenyl or phenoxy functionalization have been proposed as additives to be mixed with industry-standard PFPE disk lubricants to improve their overall properties. Materials added to thin film coatings typically modify processing and/or end-use properties. For example, additives based on the cyclotriphosphazene X-1P provides increased lubricity of the mixture PFPE films due to their lack of adhesion to the underlying carbon film [16]. However, from a chemistry perspective, additives based on

THE EXPERIMENT
INTERNATIONAL JOURNAL OF SCIENCE AND TECHNOLOGY

ISSN-2319-2119

RESEARCH ARTICLE

R.J Waltman , *TheExperiment,2017,Vol42(2),2428-2440*

X-1P provide no significant antioxidant benefits at the head-disk interface which can be readily understood on the basis of their electronic structure [17]. Similarly, the studies conducted herein on phenyl- and phenoxy-terminated PFPE end groups indicate weaker interactions with the CNx model carbon surface that could modify lubricity and/or interface properties related to possible changes in friction and/or adsorbed film structure. But these structures may not provide any significant antioxidant benefits. This is readily understood by Fig. 9. Effective antioxidants donate electrons easily and typically incorporate a highly conjugated structure to stabilize the loss of an electron by delocalization, or incorporate a phenolic structure that can accommodate the loss of an electron by resonance stabilization [18].Benzene-based end groups like ZB2 presently lack the phenolic OH groups.

Conclusions:

The adsorbed film structures of perfluoropolyethers (PFPEs) modified with benzene functional group(s) either on the chain ends or in the middle of the main chain were investigated. Surface energy as a function PFPE film thickness and of time showed the benzene functional group oriented to the PFPE/CNx surface. The orientation towards the CNx surface was kinetically much slower than OH groups despite all PFPEs having similar main chains. The bonding of the benzene functional group to the underlying carbon surface was found to be significantly weaker than OH functional groups and/or more readily removed by the solvent. Model dimer interactions via ab initio calculations showed significantly longer closest contact distances for benzene/CNx compared to OH/CNx, indicative of the weaker intermolecular interactions. Benzene rings may not provide enough adhesion to the underlying CNx surface for utilization in hard disk drive applications.

Acknowledgements:

We thank Dr. L. Bailey Jr., Dept. of Chemical Engineering, Stanford University, Stanford, CA 94305, for a sample of ZB2 (year 1999).

Figures:

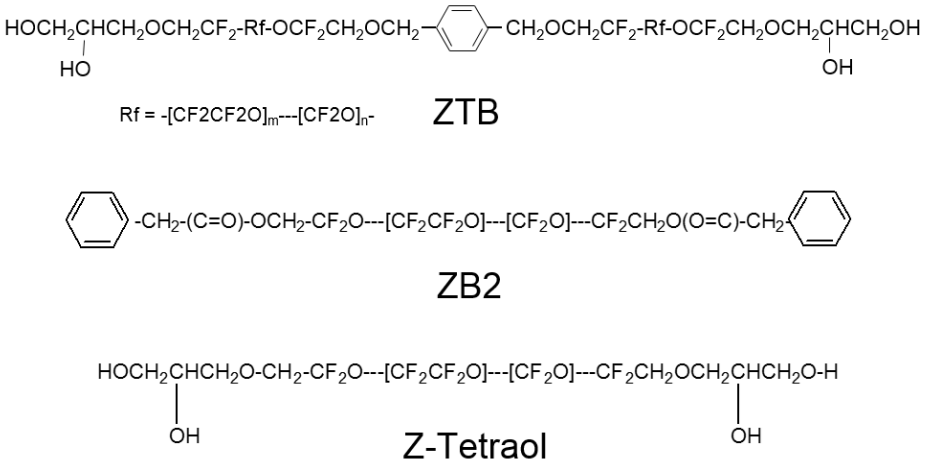

Figure 1. PFPE chemical structures.

THE EXPERIMENT
INTERNATIONAL JOURNAL OF SCIENCE AND TECHNOLOGY

ISSN-2319-2119

RESEARCH ARTICLE

R.J Waltman , *TheExperiment,2017,Vol42(2),2428-2440*

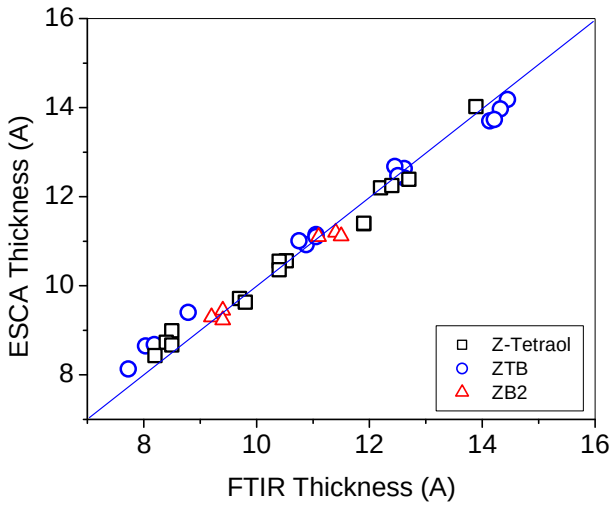

Figure 2.ESCA-FTIR film thickness calibration for Z-Tetraol, ZTB and ZB2.

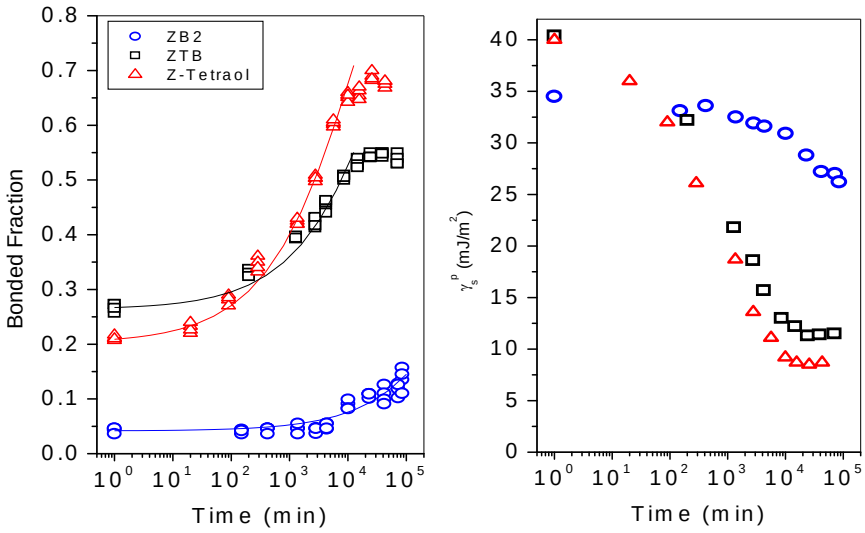

Figure 3. (Left) The changes in the PFPE bonded fraction as a function of time. (Right) The corresponding changes in the polar surface energy as a function of time. Storage and measurement conditions were ambient 20 ºC, 50 % RH. All PFPE film thicknesses are 11 – 12 Å on CNx (15 at% N).

THE EXPERIMENT
INTERNATIONAL JOURNAL OF SCIENCE AND TECHNOLOGY

ISSN-2319-2119

RESEARCH ARTICLE

R.J Waltman , *TheExperiment,2017,Vol42(2),2428-2440*

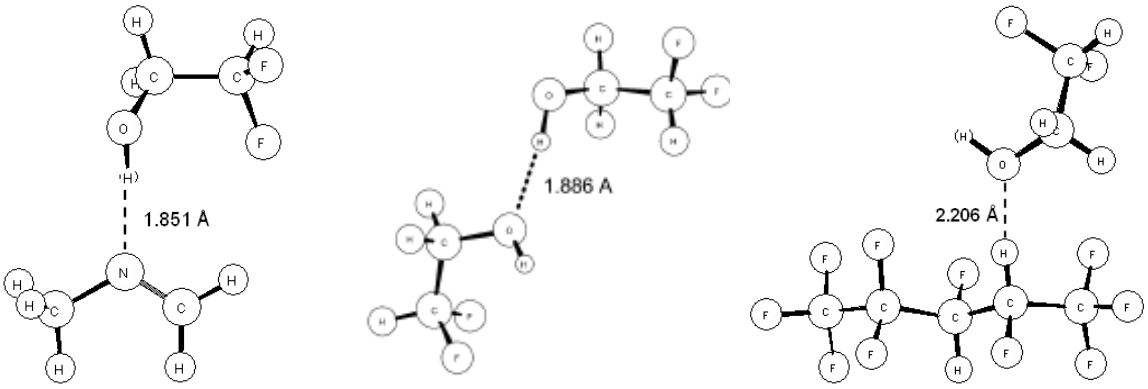

Figure 4. The B3PW91/6-311++G(d,p) optimized geometries for some model interactions between a PFPE OH end group (CFH2CH2OH) and (left) an imine carbon surface;(middle) another PFPE OH end group; and (right) Vertrel-XF. The equilibrium intermolecular distance between the PFPE OH end group and the surface polar groups are given in angstrom. No imaginary frequencies were computed for the dimers.

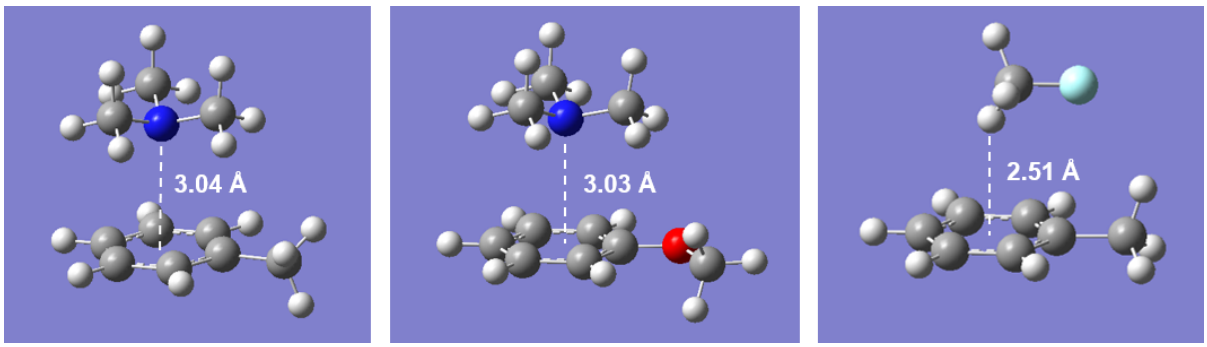

Figure 5. The MP2/6-311++G(d,p) optimized geometries for some model interactions between (left) methylbenzene and trimethylamine; (middle) methoxybenzene and trimethylamine; and (right) methylbenzene and CH_3F.The equilibrium intermolecular distances are given in angstrom. No imaginary frequencies were computed for the dimers. Trimethylamine represents a local environment of an amorphous nitorgenated carbon film. CH_3F represents the chemically salient feature of the solvent Vertrel-XF.

THE EXPERIMENT
INTERNATIONAL JOURNAL OF SCIENCE AND TECHNOLOGY

ISSN-2319-2119

RESEARCH ARTICLE

R.J Waltman , *TheExperiment,2017,Vol42(2),2428-2440*

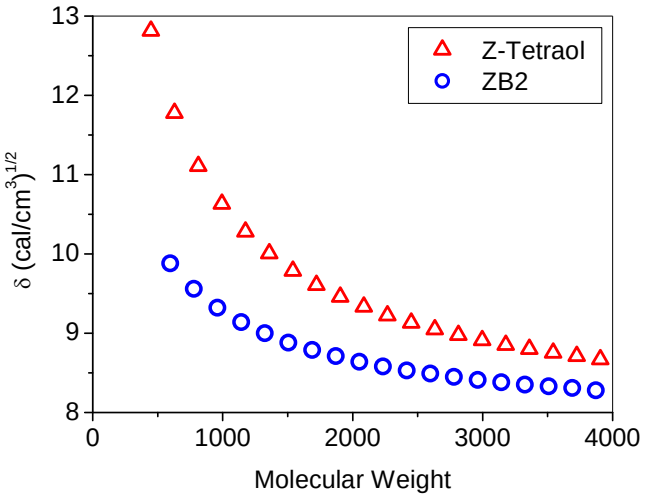

Figure 6. The calculated solubility parameter for Z-Tetraol and ZB2 as a function of molecular weight.

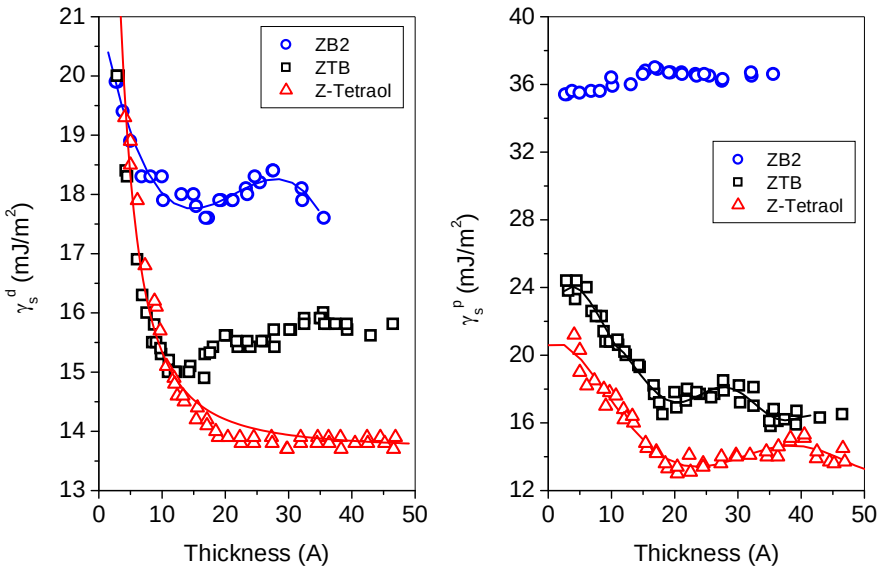

Figure 7. The experimental(left) dispersive and (right) polar components of the surface energy as a function of PFPE film thickness as determined by contact angle goniometry. The CNx films have 20 at% N.

THE EXPERIMENT
INTERNATIONAL JOURNAL OF SCIENCE AND TECHNOLOGY

ISSN-2319-2119

RESEARCH ARTICLE

R.J Waltman , *TheExperiment,2017,Vol42(2),2428-2440*

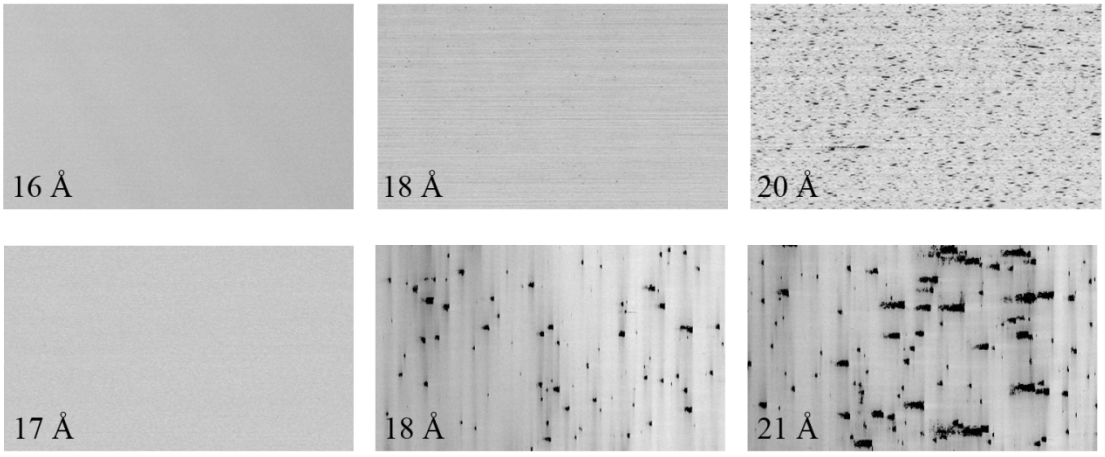

Figure 8. The experimentalOSA images as a function PFPE film thickness for: (top row) ZTB; and (bottom row) ZB2. The dark droplets are lubricant dewetting that form as a result of having exceeded the monolayer film thickness.

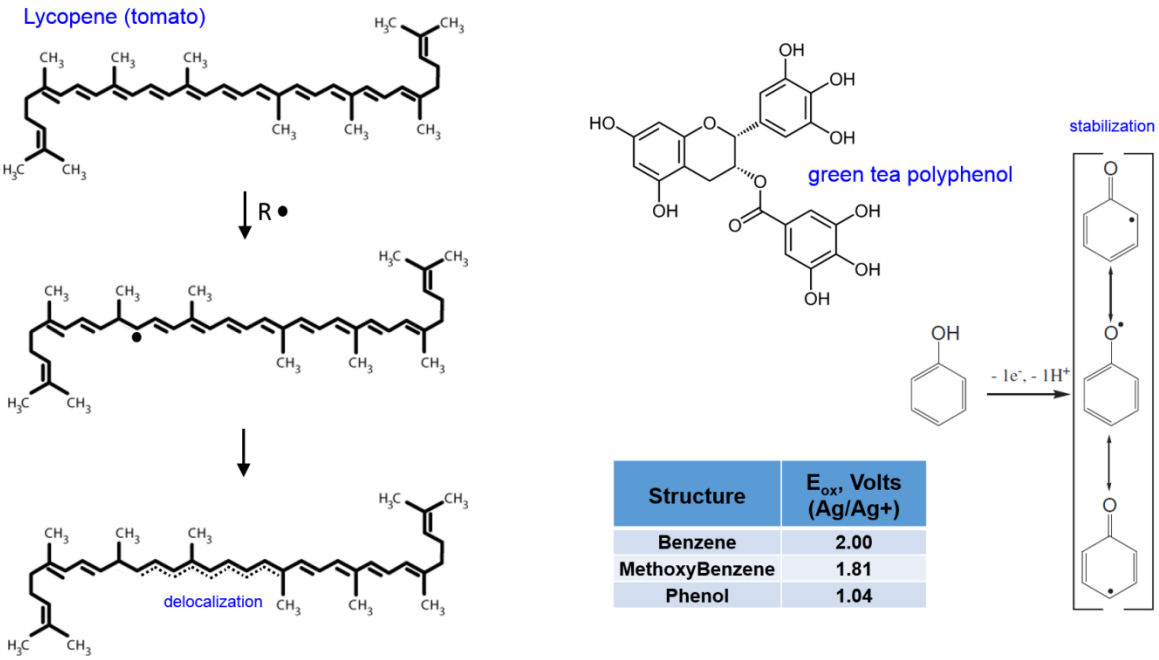

Structure	E_{ox}, Volts (Ag/Ag+)
Benzene	2.00
MethoxyBenzene	1.81
Phenol	1.04

Figure 9. The property of antioxidation is facilitated by a highly conjugated chemical structure like (left) lycopene which can delocalize the unpaired electron; and/or a phenolic structure like (right) green tea components that can be stabilized by resonance. For benzene/phenolic structures, note the significantly decreased electrochemical oxidation potential of phenol compared to benzene and methoxybenzene (see table in figure).

THE EXPERIMENT
INTERNATIONAL JOURNAL OF SCIENCE AND TECHNOLOGY

ISSN-2319-2119

RESEARCH ARTICLE

R.J Waltman , *TheExperiment,2017,Vol42(2),2428-2440*

Tables:

Table 1. NMR data for Z-Tetraol, ZTB and ZB2. Mn is the number average molecular weight.

Structure	Z-Tetraol	ZTB (per chain x 2)	ZB2
$(CF_2O)_n$; n =	10	5	12
$(CF_2CF_2O)_m$; m =	10	5.5	14
$CH_2OCH_2CH(OH)CH_2OH$	93 %	96 %	0 %
$CH_2OC(=O)$-Phenyl	0 %	0 %	100 %
n/m ratio	1.0	0.9	0.9
Mn	2200	2500	2800

Table 2. B3PW91/6-311++G(d,p) optimized hydrogen bond distance and ΔE corrected for zero-point energy contributions. Fig. 4 dimer interactions.

Dimer	Model Interaction	H-bond distance (Å)	ΔE (kcal/mol)
$HCF_2CH_2OH + CH_3N{=}CH_2$	PFPE / CNx	1.851	-6.14
$HCF_2CH_2OH + HCF_2CH_2OH$	PFPE / PFPE	1.886	-4.60
HCF_2CH_2OH + Vertrel-XF	PFPE / Solvent	2.206	-2.74

Table 3. MP2/6-311++G(d,p) optimized hydrogen bond distance and ΔE corrected for zero-point energy contributions. Fig. 5 dimer interactions.

Dimer	Model Interaction	Intermolecular distance (Å)	ΔE (kcal/mol)
Benzene + $(CH_3)_3N$	ZB2 / CNx	3.039	-5.23
Benzene + CFH_3	ZB2 / Solvent	2.508	-4.39

Table 4. Computed solubility parameter for Tetraol adducts and Vertrel-XF solvent.

Lubricant or Solvent	Molecular Weight	δ $(cal/cm^3)^{½}$
Vertrel-XF	252	6.2
Z-Tetraol	2200	9.2
ZB2	2800	8.5

Table 5. Monolayer Thickness (h_m) for Z-Tetraol, ZTB and ZB2. Mn is the number average molecular weight. N/A = Not Applicable.

	Z-Tetraol (Mn = 2200)	ZTB (Mn = 2500)	ZB2 (Mn = 2800)
OSA	22 < h_m< 24 Å	16 < h_m< 20 Å	17 < h_m< 18 Å
Surface Energy (polar minimum)	21 Å	18 Å	N/A
Surface Energy (dispersive minimum)	N/A	17 Å	18 Å
AVG	22 ± 1 Å	18 ± 1 Å	18 ± 1 Å

THE EXPERIMENT
INTERNATIONAL JOURNAL OF SCIENCE AND TECHNOLOGY

ISSN-2319-2119

RESEARCH ARTICLE

R.J Waltman , *TheExperiment,2017,Vol42(2),2428-2440*

References:

1. Waltman, R.J., Raman, V.; Burns, J. The contribution of thin PFPE lubricants to slider-disk spacing. 3. Effect of main chain flexibility. Tribol. Lett. 2004; 17: 239 - 244.
2. Waltman, R.J., Wiita, C. Main Chain Effects in Tetraol-Functionalized Perfluoropolyethers. Tribol. Online 2015; 10: 262 – 272.
3. Burns, J.M., Carter, M.D., Guo, X.-C., Marchon, B., Waltman, R.J. Lubricant with Non-terminal Functional Groups. USP 7,943,558-B2, 2011.
4. Tsuzuki, S. Interactions with Aromatic Rings. Struc. Bond 2005; 115: 149 – 193.
5. Bailey Jr, L.Dept. of Chemical Engineering, Stanford University, Stanford, CA 1999.
6. Toney, M.F., Mate, C.M., Pocker, D.J.Calibrating ESCA and Ellipsometry Measurements of Perfluoropolyether Lubricant Thickness. IEEE Trans. Magn. 1998; 34: 1774 - 1776.
7. Gaussian 98, Revision A.7**:** Frisch, M.J., Trucks, G.W., Schlegel, H.B., Scuseria, G.E., Robb, M.A., Cheeseman, J.R., Zakrzewski, V.G., Montgomery Jr., J.A., Stratmann, R.E., Burant, J.C., Dapprich, S., Millam, J.M., Daniels, A.D., Kudin, K.N., Strain, M.C., Farkas, O., Tomasi, J., Barone, V., Cossi, M., Cammi, R., Mennucci, B., Pomelli, C., Adamo, C., Clifford, S., Ochterski, J., Petersson, G.A., Ayala, P.Y., Cui, Q.;, Morokuma, K., Malick, D.K., Rabuck, A,D., Raghavachari, K., Foresman, J.B., Cioslowski, J., Ortiz, J.V., Baboul, A.G., Stefanov, B.B., Liu, G., Liashenko, A., Piskorz, P., Komaromi, I., Gomperts, R., Martin, R.L., Fox, D.J., Keith, T., Al-Laham, M.A., Peng, C.Y., Nanayakkara, A., Gonzalez, C., Challacombe, M., Gill, P.M.W., Johnson, B., Chen, W., Wong, M.W., Andres, J.L., Gonzalez, C., Head-Gordon, M., Replogle, E.S., Pople, J.A., Gaussian, Inc., Pittsburgh PA, USA.
8. Becke, A.D. Density-Functional Thermochemistry. IV. A New Dynamical Correlation Functional and Implications for Exact-Exchange Mixing. J. Chem. Phys. 1996; 104: 1040 – 1046.
9. Perdew, J.P., Burke, K., Wang, Y. Generalized Gradient Approximation for the Exchange-Correlation Hole of a Many-Electron System. Phys. Rev. B, 1996; 54: 16533 – 16539.
10. GaussView 2.1,Gaussian, Inc., PittsburghPA.
11. CambridgeSoft Chem 3D Ultra, Version 4.0, Cambridge, MA, USA.
12. Daza, M.C., Dobado, J.A., Molina, J.M., Salvador, P., Duran, M., Villaveces, J.L. Basis Set Superposition Error-Counterpoise Corrected Potential Energy Surfaces. Application to Hydrogen Peroxide- - -X (X=F^-, Cl^-, Br^-, Li^+, Na^+) Complexes. J. Chem. Phys. 1999; 110: 11806 – 11813.
13. Grulke, E.A., in Polymer Handbook, 3rd ed., Brandrup, J., Immergut, E.H., eds., John Wiley & Sons, New York 1989; 7: 519 – 520.
14. Fedors, R.F. A Method for Estimating both the Solubility Parameters and the Molar Volumes of Liquids. Polymer Eng. Sci. 1974; 14: 147 – 154.
15. Waltman, R.J. Z-Tetraol Composition and Bonding to the Underlying Carbon Film. J. Colloid Interface Science 2009; 333: 540 – 547.
16. Mate, M., Kasai, P.H., Tyndall, G.W., Lee, C.H., Raman, V., Pocker, D.J., Waltman, R.J. Investigation of Phosphazene Additive for Magnetic Recording Lubrication. IEEE Trans. Magn. 1998; 34: 1744 –1746.
17. Waltman, R.J., Lengsfield, B., Pacansky, J. Lubricants for Rigid Magnetic Media Based upon Cyclotriphosphazenes: Interactions with Lewis Acid Sites. Chem. Mater. 1997; 9: 2185 – 2196.
18. The Chemistry of Phenols, Rappoport, Z., ed., John Wiley & Sons, England 2003.

THE EXPERIMENT
INTERNATIONAL JOURNAL OF SCIENCE AND TECHNOLOGY

ISSN-2319-2119

RESEARCH ARTICLE

R.J Waltman , *TheExperiment,2017,Vol42(2),2428-2440*

Author & Affiliation

R.J. Waltman
Western Digital Company
5601 Great Oaks Parkway
San Jose, CA, USA 95119-1003